AIAA 80-1011R

Noise from a Vibrating Propeller

H. L. Runyan*
The George Washington University, Hampton, Va.

This paper is concerned with an analytical study of the noise from a vibrating propeller. The influence of airfoil thickness as well as steady loading are also included in order to provide a basis for comparison. The analysis was based on the concept of distributing sources and doublets on the surface of the blade, which were multiplied by their appropriate strength factors. The noise in the plane of the propeller was dominated by the thickness noise. When the observation point was rotated 45 deg ahead of the propeller plane, the steady-state load noise and the vibration noise were greater than the thickness noise. Moving the observer's position to the propeller axis, the thickness noise and loading noise were zero, and a pure sinusoidal noise was found, caused by the vibrations of the propeller.

Nomenclature

a	= speed of sound
A	= area
b	= half-chord
$c(x)$	= chord function
C_{L_α}	= lift coefficient
$F(\tau)$	= doublet strength
h	= bending displacement function
h_0	= bending displacement magnitude
M_t	= tip Mach number
n_0	= normal to velocity vector at x_0, θ_0, r_0
$P(t)$	= total pressure $= P_L + P_T$
P_T	= thickness pressure
P_L	= lift pressure
r_0	= radial distance of pulse to propeller axis
t	= time of arrival of pulse at field point (x,y,z)
U	= forward velocity
V	= total velocity at r_0
x_0	= source point location—distance from propeller plane—positive aft
x,y,z	= field point location
α	= angle of attack
ϵ_0	= $\tan^{-1}(U/r_0\Omega)$
$\zeta(\tau),\eta(\tau),\zeta(\tau)$	= location of source or doublet
θ_A	= geometrical angle of blade at r_0, referred to the plane of rotation
θ_0	= angular position of propeller, measured from y axis
ρ	= air density
τ	= time of doublet or source pulse
ϕ	= velocity potential
ψ	= acceleration potential
Ω	= rotational speed
ω	= blade vibration frequency

Introduction

DURING acoustical testing of several propeller blades, some of the propellers exhibited a very sharp increase in noise at certain high rotational speeds. Examination of the data indicated the possibility that the blades might be experiencing propeller flutter. The exact rotational speed at which this occurred was not known. However, some simplified flutter calculations were made and indicated that the propellers could have fluttered in the test speed range.

A search of the literature indicated no theoretical research had been done in the area of noise produced by oscillating propeller blades. It is the purpose of this report to present the results of an analytical study of the problem. The basis of the method was developed in Ref. 1, in which a study was made aimed at determining the unsteady aerodynamic forces on an oscillating propeller blade utilizing lifting surface theory and including compressibility effects. The analysis was based on linearized equations and used the acceleration potential approach.[2]

In the present study, the concept of the acceleration potential was used as a basis for determining the noise due to vibration and blade loading. Since it has been shown by Farassat,[3] that blade thickness may be a contributing factor in noise production, thickness noise for a symmetrical airfoil section was included, the analysis of which was based on the velocity potential approach.

The analysis was done for one blade, two or more blades could be treated by a proper phasing of the one-bladed results. The calculated results are given in terms of pressure time histories at an observation point that moves at the forward velocity of the propeller. The analysis applies to both near and far field problems since no distance approximations were made.

Analysis

Since the problem to be treated is linear and since we shall be considering specifically the symmetrical thickness case, the noise due to the thickness and that due to lift are uncoupled. Thus the noise due to thickness and the noise due to lift and vibration can be combined by supersposition. First the noise due to lift and vibration will be treated, then the thickness effect studied.

Derivation of Lifting and Vibration Noise

The concept of the acceleration potential will be used in determining the noise due to lift and vibration. This method was utilized in Ref. 1, where a lifting surface procedure was developed to determine the surface forces on a propeller in compressible flow. The pressure due to a source or doublet is

$$p = \rho\psi \tag{1}$$

where ψ is the acceleration potential. The expression ψ for a source that is rotating with angular velocity Ω and translating at a uniform velocity U in the negative x direction is given in Ref. 1. In Ref. 1, interest was centered on determining the forces on the blade; consequently, the field point rotated and

Presented as Paper AIAA 80-1011 at the AIAA 6th Aeroacoustics Conference, Hartford, Conn., June 4-6, 1980; submitted July 24, 1980; revision received Sept. 28, 1981.

*Associate Research Professor of Engineering, Joint Institute for Advancement of Flight Science. Associate Fellow AIAA.

translated with the same values as the source point. In the present case, we are interested in the case of a field point that is not rotating but is translating at the same velocity and direction as the source point. Thus the expression for ψ is slightly different from that presented in Ref. 1. The coordinate system is shown in Fig. 1. The angular position of the disturbance (source or doublet) is given by $\theta_0 = \Omega\tau$, the radial distance from the propeller axis to the source point is denoted by r_0. The field (or observation) point is given by x,y,z, which is moving at a velocity U in the negative x direction.

The acceleration potential Ψ of a source may be written as

$$\Psi = \frac{1}{4\pi}\frac{F(\tau)}{D} \tag{2}$$

where

$$D = s + (1/a)\left[(x-x_0)U - (t-\tau)U^2 + yr_0\Omega\sin\theta_0 - zr_0\Omega\cos\theta_0\right]$$

and

$$s = \{[(x-x_0) - (t-\tau)U]^2 + [y - r_0\cos\theta_0(\tau)]^2 + [z - r_0\sin\theta_0(\tau)]^2\}^{1/2}$$

An auxiliary equation is given below which relates the time τ, of a pulse (located at r_0, θ_0, x_0), to the time t when the signal reaches the field point (located at x,y,z).

$$(a^2 - U^2)(t-\tau) = -(x-x_0)U + \{a^2(x-x_0)^2 + (a^2-U^2)(y^2+z^2+r_0^2-2r_0) \times [y\cos\theta_0(\tau) + z\sin\theta_0(\tau)]\}^{1/2} \tag{3}$$

In order to create a pressure discontinuity across the airfoil chord, a doublet is needed and the expression for a doublet may be obtained by taking a derivative of a source in a direction normal to the velocity vector at r_0, θ_0, x_0.

For this case, the normal derivative is

$$\frac{\partial}{\partial n_0} = -\cos\epsilon_0\frac{\partial}{\partial x_0} - \frac{\sin\epsilon_0}{r_0}\frac{\partial}{\partial\theta_0} \tag{4}$$

where n_0 is the normal to the velocity vector at x_0, θ_0, r_0.

Applying this expression to Ψ results in

$$\Psi_D = \frac{\partial\Psi}{\partial n_0} = -\left(D\frac{\partial F(\tau)}{\partial n_0} - F(\tau)\frac{\partial D}{\partial n_0}\right)\Big/ 4\pi D^2 \tag{5}$$

$F(\tau)$ represents the pressure difference across the lifting surface at the location of the doublet. At this point in the analysis, $F(\tau)$ is not known. As a matter of fact it represents the unknown pressure when one is interested in solving for the pressures on a propeller by satisfying certain boundary conditions such as was done in Ref. 1. Of course, experimentally derived pressures could be inserted if they are known. For the present case, a two-dimensional pressure distribution was used for simplicity to determine $F(\tau)$. Utilizing the two-dimensional lift distribution across the chord $c(x)$, the following form is used

$$\sqrt{\frac{b-c(x)}{b+c(x)}}$$

This expression provides the shape of the pressure distribution but does not give the magnitude in pressure units. In order to determine this multiplying factor, the lift on an airfoil in its standard form is equated to the integral of the distribution multiplied by an unknown quantity B. Since the lift distribution can be integrated in closed form, B can be calculated, and thus $F(\tau)$ determined as follows:

$$\tfrac{1}{2}\rho v^2 C_{L_\alpha}\alpha A = Bb\int_{-1}^{+1}\left(\frac{1-c(x)/b}{1+c(x)/b}\right)^{1/2} \mathrm{d}[c(x)/b]$$

Integrating and solving for B results in the pressure

$$F(\tau) = 2\frac{\rho v^2}{2}C_{L_\alpha}\frac{\alpha A}{b\pi}\left(\frac{1-x_0/\cos\epsilon_0}{1+x_0/\cos\epsilon_0}\right)^{1/2} \tag{6}$$

The instantaneous angle of attack α may be written as

$$\alpha = \theta_A - \epsilon_0 - \frac{\dot{h}}{V} - \frac{\dot{\gamma}x_0}{V\cos\epsilon_0}$$

where γ is the angle of a torsion vibration mode and $\dot{\gamma}x_0/V\cos\epsilon_0$ represents an equivalent angle; θ_A is the geometric angle of the blade at r_0 measured from the plane of rotation; h is the displacement of the blade in a bending vibration mode and h/V represents an equivalent angle of attack at r_0, $x_0$2and $V^2 = r_0^2\Omega^2 + U^2$; and $\epsilon_0 = \tan^{-1}(U/r_0\Omega)$.

Assuming the vibration modes are harmonic

$$h = h_0\cos\omega_h\tau \qquad \gamma = \gamma_0\cos\omega_\gamma\tau$$

where ω_h is the bending frequency and ω_γ is the torsional frequency in

$$\alpha = \theta_A - \epsilon_0 + \frac{h_0\omega_h\sin(\omega_h\tau)}{V} + \frac{\gamma_0 x_0\omega_\gamma\sin(\omega_\gamma\tau)}{V\cos\epsilon_0} \tag{7}$$

Returning to the expression for the doublet, Eq. (5), and applying Eq. (4), results in

$$\Psi_D = \frac{1}{4\pi D^2}\left[D\left(-\cos\epsilon_0\frac{\partial F(\tau)}{\partial x_0} - \frac{\sin\epsilon_0}{r_0}\frac{\partial F(\tau)}{\partial\theta_0}\right) + F(\tau)\left(\cos\epsilon_0\frac{\partial D}{\partial x_0} + \frac{\sin\epsilon_0}{r_0}\frac{\partial D}{\partial\theta_0}\right)\right] \tag{8}$$

Examining the derivative of $F(\tau)$,

$$\frac{\partial F(\tau)}{x_0} = \frac{\partial F(\tau)}{\partial\tau}\left(\frac{\partial\tau}{\partial x_0}\right), \qquad \frac{\partial F(\tau)}{\partial\theta_0} = \left(\frac{\partial\tau}{\partial\theta_0}\right)\frac{\partial F(\tau)}{\partial\tau}$$

$$\frac{\partial F(\tau)}{\partial\tau} = 2\left(\rho\frac{V^2}{2}\right)\frac{C_{L_\alpha}}{b\pi}A\left(\frac{1-x_0/\cos\epsilon_0}{1+x_0/\cos\epsilon_0}\right)^{1/2} \times\left(\frac{h_0\omega_h^2\cos(\omega_h\tau)}{V} + \frac{\gamma_0\omega_\gamma^2\cos(\omega_\gamma\tau)}{V\cos\epsilon_0}\right)$$

The quantities $\partial\tau/\partial x_0$, $\partial\tau/\partial\theta_0$ can be determined from Eq. (3).

$$\frac{\partial\tau}{\partial x_0} = \frac{(x-x_0) - (t-\tau)U}{aD}$$

and

$$\frac{\partial\tau}{\partial\theta_0} = \frac{-y_0 r_0\sin(\Omega\tau) + zr_0\cos(\Omega\tau)}{as + (x-x_0)U - (t-\tau)U^2}$$

The remaining terms to be determined, $\partial D/\partial x_0$, $\partial D/\partial\theta_0$, are given below. The quantity D is defined following Eq. (2).

$$\frac{\partial D}{\partial x_0} = \frac{\partial s}{\partial x_0} + \frac{1}{a}\left(-U + \frac{\partial\tau}{\partial x_0}U^2 + yr_0\Omega^2\cos(\Omega\tau)\frac{\partial\tau}{\partial x_0} + z_0 r_0\Omega^2\sin(\Omega\tau)\frac{\partial\tau}{\partial x_0}\right) \tag{9}$$

where

$$\frac{\partial s}{\partial x_0} = \frac{1}{s}\left\{[(x-x_0)-(t-\tau)U]\left(U\frac{\partial \tau}{\partial x_0}-1\right)\right.$$

$$\left.+yr_0\Omega\sin\Omega\tau\frac{\partial \tau}{\partial x_0}-zr_0\Omega\cos(\Omega\tau)\frac{\partial \tau}{\partial x_0}\right\}$$

and

$$\frac{\partial D}{\partial \theta_0} = \frac{\partial s}{\partial \theta_0}+\frac{1}{a}\left(U^2\frac{\partial \tau}{\partial \theta_0}+yr_0\Omega\cos(\Omega\tau)+zr_0\Omega\sin(\Omega\tau)\right)$$

where

$$\frac{\partial s}{\partial \theta_0} = \frac{1}{s}\left\{[(x-x_0)-(t-\tau)U]U\frac{\partial \tau}{\partial \theta_0}\right.$$

$$\left.+yr_0\sin(\Omega\tau)-zr_0\cos(\Omega\tau)\right\}$$

This completes the derivation of the pressure $P_L=\rho\psi$ at a point x,y,z due to a doublet located at r_0, $x_0/\cos\epsilon_0$, θ_0. The next section is concerned with a derivation of the noise due to thickness.

Noise Due to Thickness

Bernoulli's equation may be written as

$$P_T=\rho\left(\frac{\partial \phi}{\partial t}+U\frac{\partial \phi}{\partial x}\right) \tag{10}$$

where ϕ is the velocity potential. The expression for the velocity potential ϕ is identical to that used for the acceleration potential with the exception that $F(\tau)$ is replaced by a value that is constant with regard to time, since a time variation of the source would simulate a pulsating body. Therefore

$$\phi=F/4\pi D \tag{11}$$

The strength of the source F is directly related to the velocity normal to the surface or $F=$slope$\times$stream velocity (for small slopes), or

$$F=(\mathrm{SL})(V)$$

where

$$V=(r_0^2\Omega^2+U^2)^{1/2}$$

SL is the slope of airfoil surface at location of source; the derivatives of ϕ are

$$\frac{\partial \phi}{\partial t} = -\frac{1}{4\pi}\frac{(\mathrm{SL})(V)}{D^2}\left\{\frac{\partial s}{\partial t}+\frac{1}{a}\left[\left(\frac{\partial \tau}{\partial t}-1\right)U^2\right.\right.$$

$$\left.\left.+yr_0\Omega^2\cos(\Omega\tau)\frac{\partial \tau}{\partial t}+zr_0\Omega^2\sin(\Omega\tau)\frac{\partial \tau}{\partial t}\right]\right\}$$

$$\frac{\partial s}{\partial t} = \frac{1}{s}\left\{[(x-x_0)-(t-\tau)U]U\left(\frac{\partial \tau}{\partial t}-1\right)\right.$$

$$\left.+yr_0\Omega\sin(\Omega\tau)\frac{\partial \tau}{\partial t}-zr_0\Omega\cos(\Omega\tau)\frac{\partial \tau}{\partial t}\right\}$$

where

$$\frac{\partial \tau}{\partial t} = \frac{SI}{SI+r_0y\Omega\sin(\Omega\tau)-r_0z\Omega\cos(\Omega\tau)}$$

and

$$SI=\{a^2(x-x_0)^2+(a^2-U^2)(y^2+z^2+r_0^2)$$

$$-2r_0[y\cos(\Omega\tau)+z\sin(\Omega\tau)]\}^{1/2}$$

For the derivative with respect to x,

$$\phi=\frac{1}{4\pi}\frac{(\mathrm{SL})V}{D}$$

$$\frac{\partial \phi}{\partial x}=\frac{(\mathrm{SL})(V)}{4\pi D^2}\frac{\partial D}{\partial x}$$

$$\frac{\partial D}{\partial x}=\frac{\partial s}{\partial x}+\frac{1}{a}\left(U-\frac{\partial t}{\partial x}U^2\right)$$

$$\frac{\partial s}{\partial x}=\frac{1}{s}\left\{[(x-x_0)-(t-\tau)U]\left(1-\frac{\partial t}{\partial x}U\right)\right\}$$

$$\frac{\partial t}{\partial x}=\frac{1}{a^2-U^2}\left(-U+\frac{a^2(x-x_0)}{SI}\right)$$

This completes the derivation of the thickness effects.

Computational Procedure

The pressure at a field point x,y,z will be the integral of the sum of Eqs. (1) and (10),

$$P(t)=\int_A (P_L+P_T)\,dA$$

over the area of the propeller blade at a given time t. The integration was accomplished by using a rectangular distribution in the span and chord directions. Thus the value of the integrand was calculated at a selected point on the blade and multiplied by a differential area ΔA with the selected point in the center of the area.

One complication arose owing to the necessity of properly accounting for retarded time. This was handled in the following manner. A time, τ, was chosen, which represents the time a source pulses on the blade. Corresponding to the time τ, a position was selected on the blade, which for convenience was the farthest outboard span position and located in the center of the chord ($x_0=0$). The time of arrival t at the field x,y,z of a pulse created at time τ was calculated from Eq. (3).

When the disturbance point is moved to another position on the blade, it is necessary that the pulse arrives at time t, in order to sum all the pressure pulses from all points on the blade which arrive at the same time. Therefore, with a new pulse location, it is necessary to insert the time t into Eq. (8) and solve for τ. With τ calculated, then the pressure pulse from that position on the blade can be calculated and added to the pulses from the other positions on the blade, all of which arrive at the same time t at the field point. When all the source points on the blade have been calculated and added, a new τ is selected and the entire process repeated. For the present calculation, one complete revolution of the propeller was divided into 1024 parts and consequently a time history of the pressure is obtained.

The results of sample calculations are presented in the next section. The propeller was divided into 20 chordwise pulse points and 20 spanwise sections. In order to reduce the computation time, the five spanwise stations nearest the hub were eliminated and the results were compared to the results obtained with a complete 20-station result and no appreciable difference was found. Thus the results for $20\times15=300$ integration areas were used. Since the calculations were repeated 1024 times, a total of 307,200 points were calculated. The properties of the propeller are given in Table 1.

Discussion of Results

In this section the results of calculating the noise due to thickness, lift, and vibration are given.

Table 1 Blade characteristics

Radius	= 1.30 m
rpm	= 2145
Chord	= 0.156 m
Thickness	$= T(r_0) = 0.069 + 3.2244\, e^{-8.05 r_0}$
Airfoil shape	$= (C)\,[T(r_0)]\,(3.333E - 6.5079E^2 + 3.1746E^3)$
E	$= x_0/c - \frac{1}{2}$
Aircraft speed	= 144.5 km/h
Field point (in disk plane)	= 7.28 m from propeller hub, moving with aircraft
M_t	= 0.87
C_{L_α}	$= 2\pi$

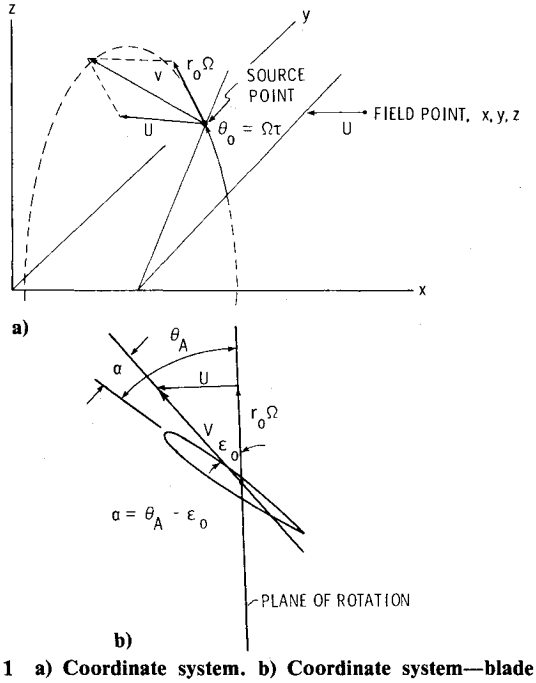

Fig. 1 a) Coordinate system. b) Coordinate system—blade cross section.

Field Point Located in Propeller Plane

Figure 2 gives the noise in the propeller plane in Newtons per square meter plotted against time t in seconds at a field point, moving at the same speed as the propeller, in the propeller disk plane and 7.28 m from propeller axis. Figure 2a presents the noise produced by thickness only. The noise is characterized by distinct positive and negative spikes with the pressure essentially zero for the remainder of the time history. To provide a comparison between the various results, the sound pressure level (SPL) is provided for each case where $P_{\text{rms}} = 0.707/2$ (peak-to-peak amplitude). For this case, SPL = 135 dB.

Figure 2b presents the noise produced by lift. For this case it was assumed that the propeller was operating with a constant 6-deg angle of attack throughout the span ($\theta_A - \epsilon_0 = 6$ deg). It is seen that a spike similar to that for thickness occurs at the same time, but the magnitude is somewhat lower than the noise owing to thickness. In addition, the pressure has a small variation with time as opposed to the thickness noise, which is virtually zero away from the spike. The SPL is 129. The total noise is shown in Fig. 2c, which is the sum of the two previous figures, where the SPL has increased to 137 dB. The Fourier transform is shown for this case in Fig. 2d. The major contribution is found in the 3rd harmonic, however the 2nd and 4th harmonics provide appreciable contributions. The Fourier transforms for the thickness and lift cases had essentially the same shapes, but each with a slightly lower magnitude.

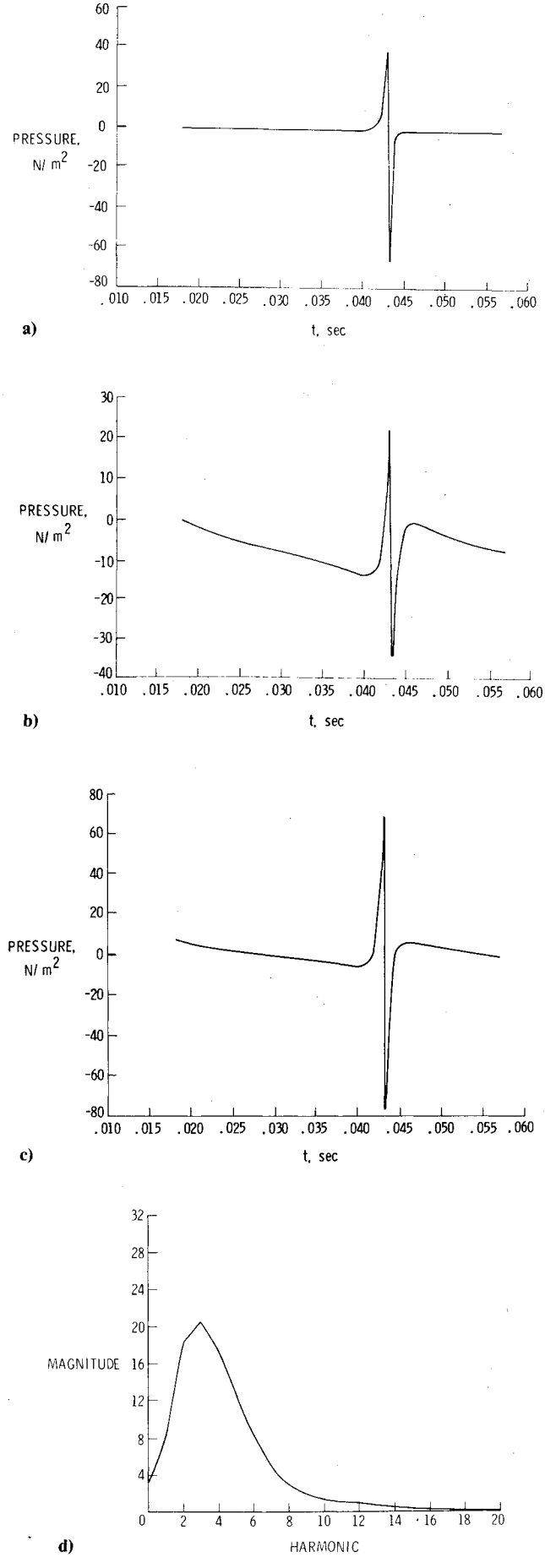

Fig. 2 a) Thickness noise—in-plane. b) Lift noise—in-plane. c) Total noise—in-plane. d) Fourier transform—total noise.

In the next figure, the effect of blade vibration is shown for the same in-plane field point location. In Fig. 3a, the time history of the noise is given for a bending vibration frequency equal to the rotational speed of the propeller. The vibration mode shape used in the calculation corresponded to that for a uniform beam, where the mass and stiffness properties were constant throughout the length of the propeller and for the first vibration mode. The tip deflection was taken as ± 0.051 m (± 2 in.). This tip amplitude assumption may be felt to be rather large; however, for the case of flutter it is thought to be within the possible amplitude range. Under normal operating conditions, a much smaller tip amplitude would probably be encountered, and hence a lower noise level would be found, and an example of a smaller tip deflection is given later. Returning to Fig. 3a, comparing the time history to Fig. 2c, two effects are noted. First, the noise is following a general sinusoidal shape when observed over the complete cycle, and second, the magnitude of the positive and negative peaks has been slightly reduced, thus indicating a surprising beneficial effect. The SPL is 135, slightly less than the result without vibration.

For the next case, the vibration frequency was increased to twice the rotational speed, Fig. 3b. Again, the overall vibration pattern can be seen, but the peak amplitudes have been more drastically changed. The positive peak has been significantly reduced by the vibration, but the negative peak has been greatly increased. The SPL has been increased to 137 dB.

It should be realized that the phasing of the vibration mode relative to the rotational position is a selected input and changes in this phase relationship could change the magnitudes of the peak amplitudes.

For the final frequency, results for a vibration frequency that is four times the rotational speed are given in Fig. 3c. The overall time history again shows the sinusoidal noise pattern, but the peaks have again been drastically altered. The SPL is 146. The positive peak is about seven times that for the previous case ($\omega_h = 2\Omega$), whereas the negative peak has been just slightly magnified. The Fourier transform for this case is given in Fig. 3d. As would be expected, the power is concentrated at the 4th harmonic corresponding to the input vibrational frequency.

To illustrate the effect of a smaller vibration amplitude, this case was repeated, with the amplitude reduced by a factor of 10, thus the tip deflection is ± 0.0051 m (± 0.2 in.), an amplitude which could be realized in an operational propeller. The time history is given in Fig. 3e. The effect of the reduction in which amplitudes are reduced by a factor of 10 is apparent when comparing this result to Fig. 3c. The SPL is reduced to 138, which compares to 146 for the large deflection case. Comparing this smaller vibration case to the steady case (Fig. 2c) shows that the SPL was increased by only 1 dB, and the Fourier transforms (not shown) are almost identical, the greatest power remaining in the 3rd harmonic.

Field Point Located 45 deg Ahead of Propeller Plane

For the next case, the field or observation point has been swung on a constant radius to a point ahead of the propeller at an angle of 45 deg. The time history for the thickness noise is given in Fig. 4a. The positive and negative peaks have both been drastically reduced and, also, the peaks are substantially rounded. For this case the SPL has been reduced to 105 dB. For instance, compare this result to that for the in-plane case of Fig. 2a, where the SPL was 135 dB. The lift noise is given in Fig. 4b. Although the positive peak increased, the peaks are well rounded and it is estimated that the perceived noise would also be reduced relative to the in-plane case. The SPL for this case is 120 dB, whereas the SPL for the in-plane lift case was 129 dB. The next figure of this group (Fig. 4c) contains the total noise, including the vibration noise, for $\omega_h = 4\Omega$ and the tip amplitude held at 0.051 m. The positive

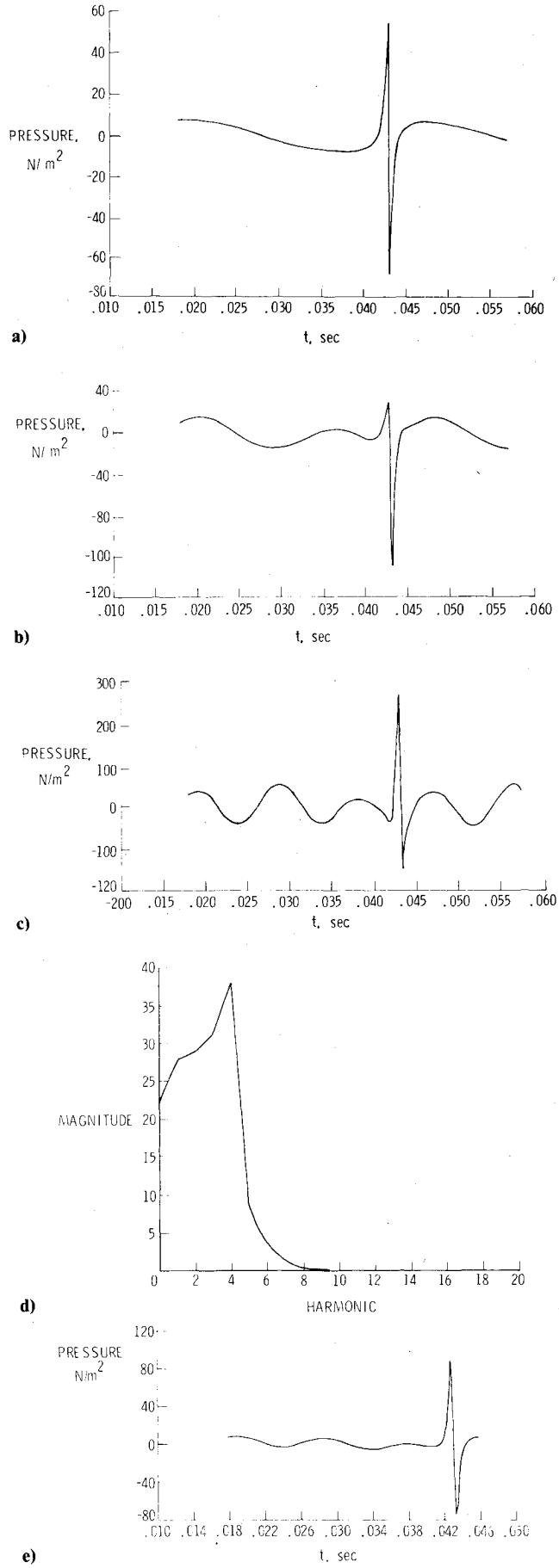

Fig. 3 a) Total noise—in-plane, $\omega_h = \Omega$. b) Total noise—in-plane, $\omega_h = 2\Omega$. c) Total noise—in-plane, $\omega_h = 4\Omega$. d) Fourier transform—in-plane, $\omega_h = 4\Omega$. e) Total noise—in-plane, $\omega_h = 4\Omega$; tip deflection = 0.0051 m.

noise peak is approximately three times that shown in Fig. 3c, but again the peaks are broader and more rounded. The SPL for this condition is 157, again, well above that for the in-plane case.

Field Point Located on Propeller Axis

The final case treated involves moving the observation point forward to the axis of the propeller or 90 deg from the plane of the propeller. Calculations for a tip deflection of 0.051 m and $\omega_h = 4\Omega$ indicate that neither the airfoil thickness nor steady lift contribute to noise. On the other hand, the noise due to vibration (Fig. 5) showed a constant amplitude, sinusoidal noise. Therefore measurements of noise on the propeller axis should indicate whether a propeller is vibrating or responding dynamically to some distributing input such as turbulence or random loading.

Additional Calculations

Other calculations have been made but were not included owing to space limitation. For instance, a torsion vibration mode shape was used for one case and it was found, at least for that case, that the in-plane noise level was so low compared to the bending vibration noise that noise due to torsional motion could be neglected.

A second bending mode was also run, and the results indicated that the noise level was somewhat below that of the first bending mode.

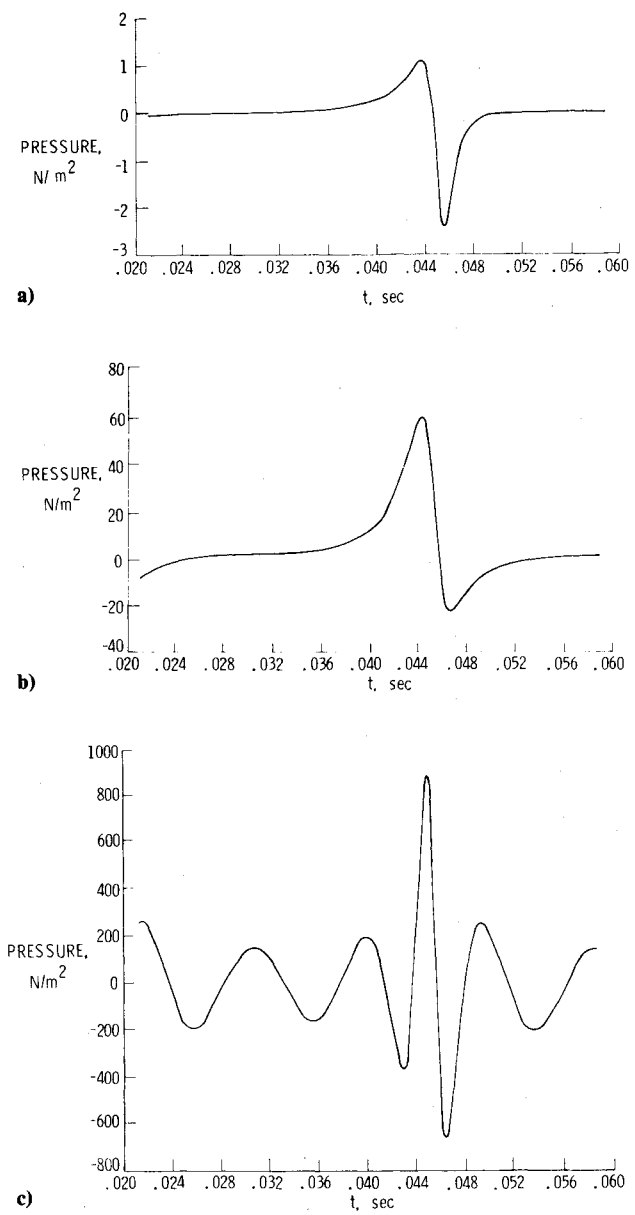

Fig. 4 a) Thickness noise—45-deg azimuth. b) Lift noise—45-deg azimuth. c) Total noise—45-deg azimuth, $\omega_h = 4\Omega$.

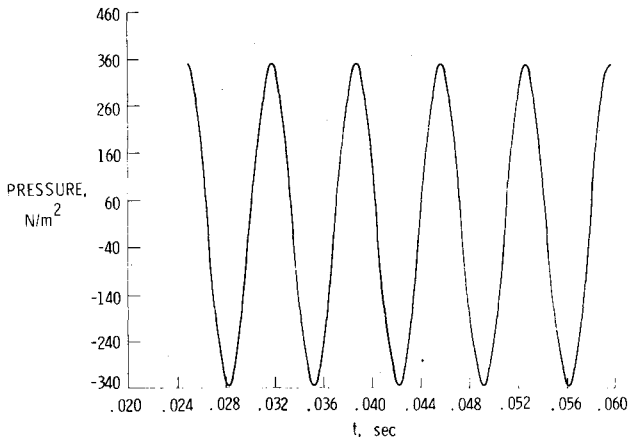

Fig. 5 Total noise—on propeller axis, $\omega_h = 4\Omega$; tip deflection = 0.051 m.

Concluding Remarks

A calculation procedure has been developed to determine the noise from a vibrating propeller. Included also is the effect of steady loading and airfoil thickness for a symmetrical airfoil section.

For the particular case studied, the in-plane noise is dominated by thickness noise, with lift and vibratory noise secondary.

Two vibration amplitudes were treated. One, corresponding to an amplitude which might be experienced during flutter, and a second which could be experienced during normal operations of the propeller. The large amplitude [tip amplitude = +0.051 m (±4 in.)] produced noise that, for the higher frequencies, dominates the noise production. However, for the case where the vibration amplitude was reduced by a factor of 10, very little effect was found on the total noise production as compared to the thickness and lift noise.

When the observation point is rotated 45 deg on a constant radius to a point ahead of the propeller plane, steady loading and vibration noise dominates and the thickness noise is negligible.

For the case of the observation point being rotated to 90 deg, i.e., on the propeller axis, both the thickness and steady loading noise are zero, and a constant amplitude, sinusoidal noise results. Thus measurements made on the propeller rotation axis should indicate noise due only to vibration or dynamic response modes.

Acknowledgment

Research funded under NASA Contract NAS1-14605-13.

References

[1] Runyan, H.L., "Unsteady Lifting Surface Theory Applied to a Propeller and Helicopter Rotor," Ph.D. Thesis, Loughborough University of Technology, Great Britain, July 1973.

[2] Dowell, E.H., Curtiss, H.C. Jr., Scanlan, R. H., and Sisto, F., *A Modern Course in Aeroelasticity*, Sijthoff and Noordhoff, the Netherlands, 1978.

[3] Farassat, F. and Brown, T.J., "A New Capability for Predicting Helicopter Rotor and Propeller Noise Including the Effect of Forward Motion," NASA TMX-74037, June 1977.